


## Improving the performance of crystalline Si solar cell by high-pressure hydrogenation

Xi-Yuan Dai(戴希远), Yu-Chen Zhang(张宇宸), Liang-Xin Wang(王亮兴), Fei Hu(胡斐), Zhi-Yuan Yu(于志远), Shuai Li(李帅), Shu-Jie Li(李树杰), Xin-Ju Yang(杨新菊), Ming Lu(陆明)

**Citation:**Chin. Phys. B . 2020, 29(11): 118801 . **doi:** 10.1088/1674-1056/abb3e3
Journal homepage: http://cpb.iphy.ac.cn; http://iopscience.iop.org/cpb

**What follows is a list of articles you may be interested in**

---

## The effect of Mn-doped ZnSe passivation layer on the performance of CdS/CdSe quantum dot-sensitized solar cells

Yun-Long Deng(邓云龙), Zhi-Yuan Xu(徐知源), Kai Cai(蔡凯), Fei Ma(马飞), Juan Hou(侯娟), Shang-Long Peng(彭尚龙)
Chin. Phys. B . 2019, 28(9): 098802 . **doi:** 10.1088/1674-1056/ab37f3

## Detection of finger interruptions in silicon solar cells using photoluminescence imaging

Lei Zhang(张磊), Peng Liang(梁鹏), Hui-Shi Zhu(朱慧时), Pei-De Han(韩培德)
Chin. Phys. B . 2018, 27(6): 068801 . **doi:** 10.1088/1674-1056/27/6/068801

## Application of millimeter-sized polymer cylindrical lens array concentrators in solar cells

Yao-Ju Zhang(张耀举), Yi-Jie Li(李艺杰), Jie Lin(林洁), Chao-Long Fang(方朝龙), Si-Yuan Liu(刘思远)
Chin. Phys. B . 2018, 27(5): 058801 . **doi:** 10.1088/1674-1056/27/5/058801

## Boron implanted emitter for n-type silicon solar cell

Liang Peng, Han Pei-De, Fan Yu-Jie, Xing Yu-Peng
Chin. Phys. B . 2015, 24(3): 038801 . **doi:** 10.1088/1674-1056/24/3/038801

## Light scattering effect of submicro-textured Ag/Al composite films prepared at lower substrate temperatures

Tang Ping-Lin, Wu Yong-Gang, Tong Guang-De, Xia Zi-Huan, Liu Ren-Chen, Liang Zhao-Ming, Zhou Jian
Chin. Phys. B . 2013, 22(7): 078801 . **doi:** 10.1088/1674-1056/22/7/078801

---

# Improving the performance of crystalline Si solar cell by high-pressure hydrogenation*

Xi-Yuan Dai(戴希远)[1], Yu-Chen Zhang(张宇宸)[1], Liang-Xin Wang(王亮兴)[2], Fei Hu(胡斐)[1], Zhi-Yuan Yu(于志远)[1], Shuai Li(李帅)[1], Shu-Jie Li(李树杰)[3], Xin-Ju Yang(杨新菊)[3], and Ming Lu(陆明)[1,†]

[1] *Department of Optical Science and Engineering and Shanghai Ultra-Precision Optical Manufacturing Engineering Center, Fudan University, Shanghai* 200433, *China*

[2] *School of Microelectronics, Fudan University, Shanghai* 200433, *China*

[3] *Department of Physics, Fudan University, Shanghai* 200433, *China*

(Received 1 April 2020; revised manuscript received 21 August 2020; accepted manuscript online 1 September 2020)

We report an approach of high-pressure hydrogenation to improve the performance of crystalline Si (c-Si) solar cells. As-received p-type c-Si wafer-based PN junctions were subjected to high-pressure (2.5 MPa) hydrogen atmosphere at 200 °C, followed by evaporating antireflection layers, passivation layers, and front and rear electrodes. The efficiency of the so prepared c-Si solar cell was found to increase evidently after high-pressure hydrogenation, with a maximal enhancement of 10%. The incorporation of hydrogen by Si solar cells was identified, and hydrogen passivation of dangling bonds in Si was confirmed. Compared to the regular approach of hydrogen plasma passivation, the approach of high-pressure hydrogenation reported here needs no post-hydrogenation treatment, and can be more convenient and efficient to use in improving the performances of the c-Si and other solar cells.

**Keywords:** high-pressure hydrogenation, Si solar cell, bulk passivation

**PACS:** 88.40.jj, 88.40.hj, 73.50.Gr **DOI:** 10.1088/1674-1056/abb3e3

## 1. Introduction

Crystalline Si (c-Si) solar cells are dominating the world's photovoltaic marketplace, despite the emergence of other promising solar cells such as Cu–In–Ga–Se (CIGS), CdTe, amorphous Si (a-Si) thin film, GaAs, and perovskite ones, due to their long-term stable performances and mature manufacturing processes.[1–6] Although the photoelectric conversion efficiency of the c-Si solar cell in the laboratory has been approaching its theoretical limit,[7–9] for commercial c-Si solar cells, there is still much room to improve their performances by further reducing optical and electrical losses and extending the wavelength range of photovoltaic response in cost-effective manners.[10–15] The approach of hydrogen plasma passivation has usually been used to enhance the photocharge transport by passivating bulk dangling bonds in the a-Si, c-Si, and other solar cells.[16–27] However, approaches of this kind would bring severe ion-radiation damages to solar cells, which degrade the performance of a solar cell. Therefore, post-hydrogenation treatment is needed to eliminate the negative effect of hydrogen plasma passivation. In our recent work on developing all-Si lasers,[28,29] an approach of high-pressure hydrogenation was proposed, aiming at thorough passivation of dangling bonds of Si nanocrystals and considerably enhancing their optical gains. This approach was proved to work there. Considering its effectiveness in passivating Si dangling bonds at relatively low temperatures (∼ 200 °C) without causing structural damages and hence with no need for post-hydrogenation treatment, we applied high-pressure hydrogenation in this work as an alternative to other approaches, and hoped for a more convenient and efficient way of hydrogen passivation to improve the performance of Si solar cell.

## 2. Experiments

### 2.1. Preparation of silicon solar cells

Textured p-type c-Si wafer-based PN junctions (JA Solar) are used to fabricate Si solar cells. It is ultrasonically cleaned in alcohol for 10 min and dried with nitrogen. High-pressure hydrogenation is then applied by exposing the cleaned PN junction to 2.5 MPa pure hydrogen atmosphere in an autoclave (FYXD-0.5, Dalian Tongchan) for days at 200 °C. Antireflection coatings (ARC) formed by 10 nm $SiO_2$, 50 nm $TiO_2$, and 96 nm $SiO_2$ and an 80 nm thick indium-tin-oxide (ITO) transparent conducting layer are deposited onto the front surface of PN junction sequentially. At the rear side, a 20 nm thick $Al_2O_3$ passivation layer is evaporated, followed by depositing 2 μm thick Al electrode. All the depositions of oxides are conducted by electron beam heating in a home-made evaporation system with a base pressure lower than $5 \times 10^{-4}$ Pa at the rate of 0.2 nm/s for ITO and 0.1 nm/s for $SiO_2$, $TiO_2$, and $Al_2O_3$. Finally, annealing in a nitrogen atmosphere at 500 °C for 3 min is conducted to form Ohmic contacts and to complete

*Project supported by the National Natural Science Foundation of China (Grant No. 62075044), the Shanghai Science and Technology Committee, China (Grant No. 18JC1411500), and the CIOMP–Fudan University Joint Foundation (Grant No. FC2017-001).

†Corresponding author. E-mail: minglu55@fudan.edu.cn

© 2020 Chinese Physical Society and IOP Publishing Ltd 

the fabrication of solar cells with 1 cm × 1 cm in size.

### 2.2. Measurements

The current density–voltage ($J$–$V$) characteristics and photovoltaic parameters of solar cells are measured on a solar simulator (94023A, Oriel/Newport) under AM1.5G condition. External quantum efficiency (EQE) of the solar cell is obtained by a QE/IPCE system of Oriel/Newport. The sheet resistance of PN junction before or after high-pressure hydrogenation is measured by a multifunctional four-probe tester (ST2258C, Suzhou Jingge Electronics). To identify the effect of high-pressure hydrogenation on the surface morphology, minority carrier lifetime, and hydrogen absorption, the p-type c-Si(100) wafer (two-side polished, 1–10 Ω·cm) after high-pressure hydrogenation treatment is used for characterization. The surface morphology is characterized by atomic force microscopy (AFM; Multimode V, Bruker Nano Surfaces). The composition distribution is measured by energy dispersive x-ray spectroscopy (EDX; Aztec X-Max$^N$ 80, Oxford Instruments). The reflectance spectrum is measured by spectrophotometer (Ideaoptics, PG2000-Pro-EX) with an integrating sphere. The minority carrier lifetime is acquired by measuring photoconductivity decay curves (WT-2000, Semilab). The Fourier transform infrared spectrum (FTIR) is obtained by spectrophotometer (Nicolet iS5, Thermo Fisher). The crystal structures of Si(100) wafer are examined by x-ray diffraction (XRD, Rigaku Ultima IV) with Cu $K_\alpha$ radiation.

## 3. Results and discussion

Figure 1 shows a schematic diagram of the cross-sectional structure of the c-Si solar cell used in this work. The as-received p-type Si based PN junction samples have been textured at the front surface. We passivate the rear surface with 20 nm thick $Al_2O_3$ layers,[30] followed by evaporating antireflection coatings and ITO as the front electrode and Al as the rear one.

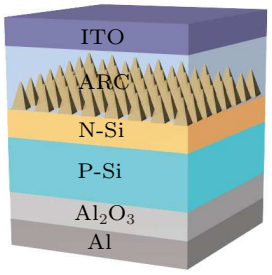



**Fig. 1.** The cross-sectional structure of the c-Si solar cell.

In Figs. 2(a)–2(c), the AFM images of Si(100) wafer surfaces after 0-, 6-, and 9-day high-pressure hydrogenation are given, respectively. Tiny spots or islands are found on the Si surface after high-pressure hydrogenation, and the longer the hydrogenation time, the more the number of islands was. However, the hydrogenated Si surface remains shining in appearance, and the surface roughness for 0-, 6-, and 9-day hydrogenation was 0.448 nm, 0.749 nm, and 0.991 nm, respectively. The EDX characterization shows that the islands were composed of Si, as shown in Fig. 2(d). The formation of the Si islands could be attributed to the enhanced surface diffusion of Si atoms after hydrogenation,[31,32] which facilitates the formation of Si atomic clusters at the surface nucleation sites. Figure 3 gives the reflection spectra of Si(100) wafer surfaces and PN junction after 0- and 6-day high-pressure hydrogenation. No obvious difference in reflectivity is found before and after high-pressure hydrogenation.

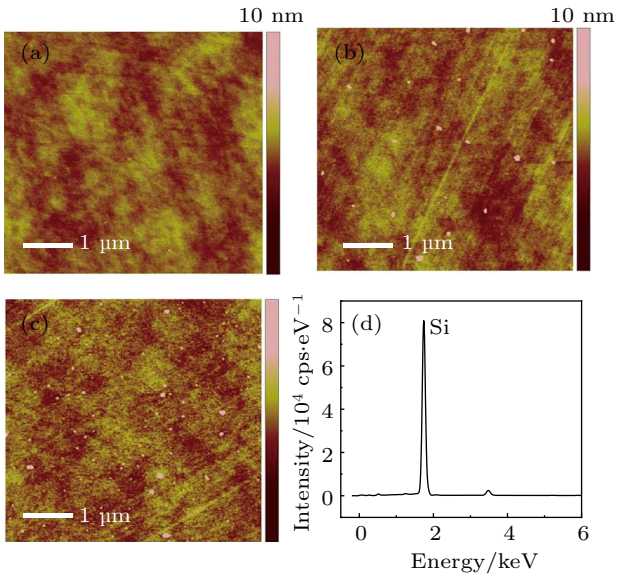



**Fig. 2.** (a)–(c) The AFM images of Si(100) wafers of 0-, 6-, and 9-day high-pressure hydrogenation, respectively. (d) The EDX spectrum of islands on the hydrogenated surface.

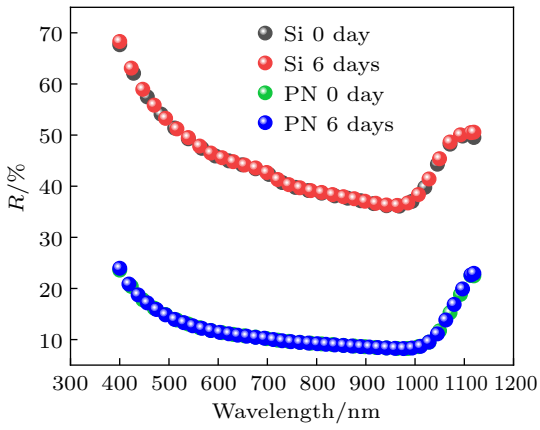



**Fig. 3.** Reflection spectra of Si(100) surfaces and PN junction after 0- and 6-day high-pressure hydrogenation.

Figures 4(a) and 4(b) give the typical $J$–$V$ and the EQE curves of c-Si solar cells after 0-, 3-, 6-, and 9-day high-pressure hydrogenation, respectively. The photovoltaic parameters for all the solar cell samples are given in Table 1. The efficiency data are plotted in Fig. 5. It is seen that the efficiency increases steadily at first with increasing hydrogenation

time, reaches the maximum at around 6-day hydrogenation with 10% enhancement as compared to the 0-day cell, and then goes down. The trend of change in short-circuit current density agrees with that of conversion efficiency, indicating that recombination is suppressed by hydrogenation. The EQE values evolve similarly to that of conversion efficiency in the whole responsive wavelength range, without reforming the shape of the EQE spectrum considerably, that is, unusual change at the short or longwavelength regimes in the EQE curve is not found.[10,12,14] This indicates that the bulk recombination rather than the surface one is mainly suppressed by the high-pressure hydrogenation.[10,12,14] Furthermore, after high-pressure hydrogenation for up to 6 days, the $R_s$ decreases and the $R_{sh}$ increases with the increasing hydrogenation time. However, for the hydrogenation time of 9 days, the $R_s$ increases and the $R_{sh}$ decreases. These trends of the $R_s$ and $R_{sh}$ evolution correlate with that of $J$ similarly, showing that the high-pressure hydrogenation does help to improve the performance of Si solar cells. But the overloading of hydrogen is detrimental. This could be due to the dissociation of Si–H bonds and the formation of hydrogen platelets when hydrogen is over incorporated, as will be discussed below. It is found in Table 1 that $V_{OC}$ decreases with the increasing hydrogenation. This could be caused by the lattice deformation due to the incorporation of interstitial hydrogen atoms and molecules,[33,34] as will be shown below. Therefore, the compromise among photovoltaic parameters to optimize the solar cell efficiency has to be considered for the high-pressure hydrogenation treatment. Also, the results of sheet resistance as a function of hydrogenation time is shown in Table 2. Within the range of error, the sheet resistance changes little. This is quite different from the case of plasma hydrogenation where large increases of surface roughness and sheet resistance usually occur.[35]

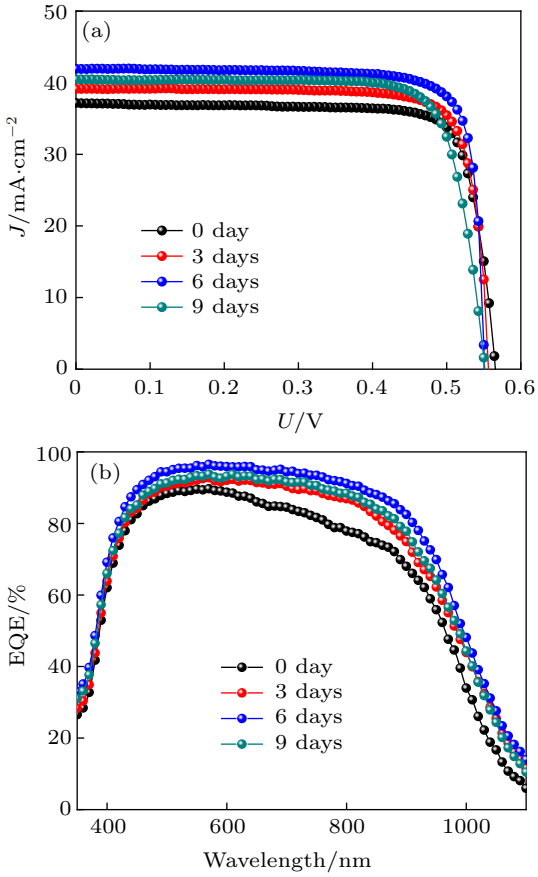



**Fig. 4.** (a) Current density–voltage characteristics, (b) the EQE curves of the c-Si solar cells with 0-, 3-, 6-, and 9-day high-pressure hydrogenation.

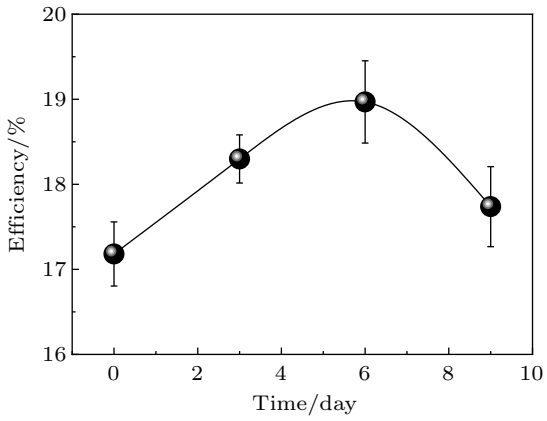



**Fig. 5.** Efficiency of the c-Si solar cells versus high-pressure hydrogenation time.

**Table 1.** Photovoltaic parameters of solar cells with different high-pressure hydrogenation time.

| Sample | $J$/mA·cm$^{-2}$ | $V_{OC}$/mV | $FF$/% | $\eta$/% | $R_s$/Ω | $R_{sh}$/Ω |
|---|---|---|---|---|---|---|
| 0-day | 37.3 ± 0.2 | 563 ± 3 | 82.2 ± 1.9 | 17.2 ± 0.4 | 1.0 ± 0.4 | 798 ± 341 |
| 3-day | 39.3 ± 0.4 | 556 ± 3 | 83.7 ± 1.8 | 18.3 ± 0.3 | 0.7 ± 0.2 | 1005 ± 274 |
| 6-day | 42.1 ± 0.6 | 551 ± 3 | 81.9 ± 2.2 | 19.0 ± 0.5 | 0.5 ± 0.1 | 1420 ± 460 |
| 9-day | 40.3 ± 1.1 | 549 ± 2 | 80.0 ± 2.8 | 17.7 ± 0.5 | 0.8 ± 0.2 | 1009 ± 419 |

**Table 2.** The sheet resistance of PN junction after different high-pressure hydrogenation time.

| Sample | 0 day | 3 days | 6 days | 9 days |
|---|---|---|---|---|
| Sheet resistance/Ω·sq$^{-1}$ | 24.9 ± 1.7 | 26.7 ± 1.6 | 25.4 ± 1.8 | 25.8 ± 1.8 |

Figure 6 gives the measured minority carrier lifetimes of Si(100) wafers after 0-, 1-, 3-, 6-, and 9-day high-pressure hydrogenation. The trend of a lifetime in Fig. 6(b) also agrees with that of the conversion efficiency. In order to assess the hydrogen incorporation by high-pressure hydrogenation and find a general physical picture behind the evolution of conversion efficiency along with those of short-circuit current density, the EQE value, minority carrier lifetime, and FTIR spectra are measured. The absorbance difference spectra are given

in Fig. 7(a). The absorbance difference is performed between Si(100) wafers with and without high-pressure hydrogenation. The spectra between 2300 $cm^{-1}$ to 2400 $cm^{-1}$ have been attributed to Si–H bonds,[36,37] whose integrated intensity can be taken as an indicator of the degree of hydrogen passivation of Si dangling bonds. Figure 7(b) shows the integrated intensity of the difference spectrum as a function of the hydrogenation time. It is seen that the degree of hydrogen passivation evolves similarly to the conversion efficiency and the other parameters. Since the high-pressure hydrogenation is conducted at 200 °C, prolonged hydrogenation could dissociate some Si–H bonds and form hydrogen platelets from the viewpoint of energetics.[26,38] Both the dissociation of Si–H bonds, hence the degradation of bulk passivation, and the formation of hydrogen platelets, would reduce the minority carrier lifetime, making the photocurrent, the corresponding EQE, and finally the conversion efficiency decrease.[26] It needs to point out that if one applies hydrogenation with hydrogen pressure higher than the ultimate one (2.5 MPa) permitted by the autoclave used in this work, the hydrogenation time would be reduced for a desired hydrogen exposure amount, and the efficiency could be further enhanced due to the decrease of hydrogenation time.

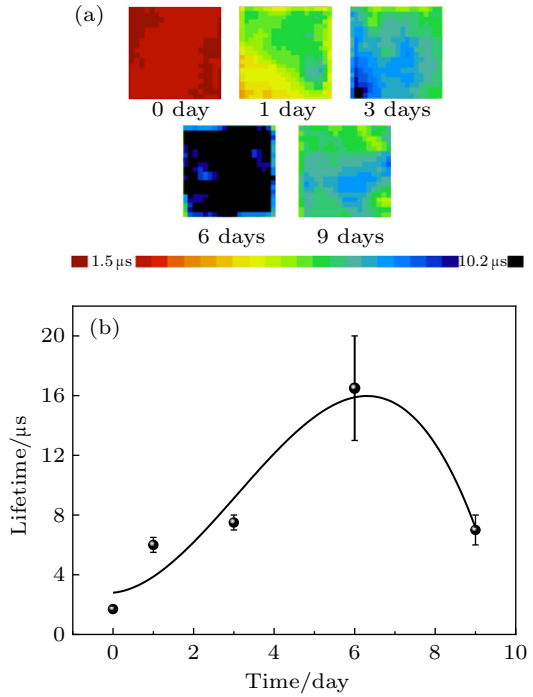



**Fig. 6.** (a) Scan image of minority carrier lifetimes of Si(100) wafers after 0-, 1-, 3-, 6-, and 9-day high-pressure hydrogenation. (b) Minority carrier lifetime versus high-pressure hydrogenation time.

The mechanism of high-pressure hydrogenation is in fact complex, but in general, the higher density of defects a solar cell possesses, the more effectively the performance of the solar cell is improved by hydrogen passivation.[27] The approach of high-pressure hydrogenation includes processes not only of saturating dangling bonds, but of freeing hydrogen atoms or molecules from the sample and generating hydrogen related defects as well.[23,26,33,39] Figure 8 shows the XRD spectra of Si(100) wafers after high-pressure hydrogenation for different days. The peak at 69.0° is attributed to the characteristic reflection of crystalline Si(400) from Si(100). It is observed that longer hydrogenation time shifts the peak angle to a higher side. For samples after 3-, 6-, and 9-day hydrogenation, the peak shifts for that without passivation by 0.18°, 0.20°, and 0.34°, respectively. This result indicates that the incorporation of interstitial hydrogen can gradually increase the lattice distortion and lower the crystalline quality,[40–42] which explains the decreasing $V_{OC}$ in the cell device.[33,34]

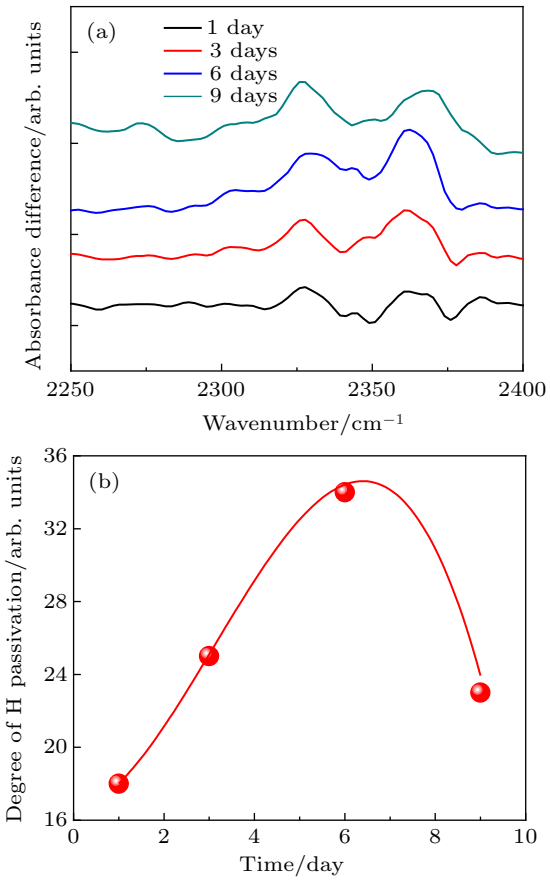



**Fig. 7.** (a) FTIR absorbance difference spectra. (b) Degree of hydrogen passivation versus high-pressure hydrogenation time.

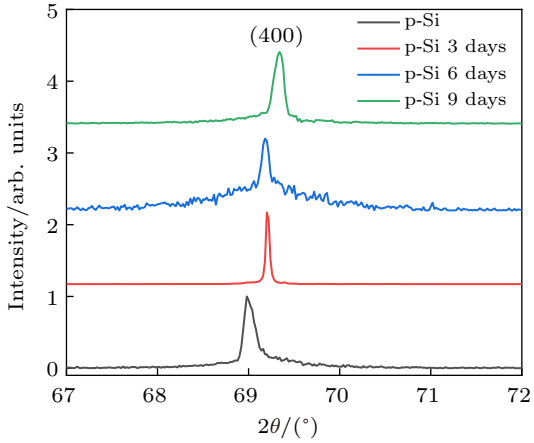



**Fig. 8.** The XRD spectra of Si(100) wafers after 0-, 3-, 6-, and 9-day high-pressure hydrogenation.

## 4. Conclusion

In this work, we report an approach of high-pressure hydrogenation to improve the performance of the c-Si solar cell by passivating Si bulk defects and facilitating the photo charge transport. Under the current experimental condition, a maximal 10% enhancement of photoelectric conversion efficiency is achieved. This approach could be more convenient and efficient to use to enhance the efficiency of Si and other solar cells if higher hydrogen pressure and proper hydrogenation time are applied.

## Acknowledgment

The authors would thank Shi-Zheng Li for minority carrier lifetime measurement.

## References

[1] Nijs J F, Szlufcik J, Poortmans J, Sivoththaman S and Mertens R P 2001 *Sol. Energ. Mat. Sol. C* **65** 249
[2] Saga T 2010 *NPG Asia Mater.* **2** 96
[3] Ribeyron P 2017 *Nat. Energy* **2** 17067
[4] Goetzberger A, Hebling C and Schock H 2003 *Materials Science and Engineering: R: Reports* **40** 1
[5] Miles R W 2006 *Vacuum* **80** 1090
[6] Sharma S, Jain K K and Sharma A 2015 *Materials Sciences and Applications* **6** 1145
[7] Lee Y, Park C, Balaji N, Lee Y J and Dao V A 2015 *Isr. J. Chem.* **55** 1050
[8] Haase F, Hollemann C, Schaefer S, Merkle A, Rienaecker M, Krügener J, Brendel R and Peibst R 2018 *Sol. Energ. Mat. Sol. C* **186** 184
[9] Green M A, Emery K, Hishikawa Y, Warta W and Dunlop E D 2015 *Progress in Photovoltaics: Research and Applications* **23** 1
[10] Wang L, Zhou Z, Hao H and Lu M 2016 *Nanotechnology* **27** 425207
[11] Zarmai M T, Ekere N N, Oduoza C F and Amalu E H 2015 *Appl. Energ.* **154** 173
[12] Zhou Z, Wang L, Shi W, Sun S and Lu M 2016 *Nanotechnology* **27** 145203
[13] Zhou Z, Hu F, Zhou W, Chen H, Ma L, Zhang C and Lu M 2017 *Nanoscale Res. Lett.* **12** 623
[14] Hu F, Zhou Z, Ma L, Zhang C, Zhou W and Lu M 2017 *Physica E* **94** 174
[15] Wang L, Zhou Z, Zhang T, Chen X and Lu M 2016 *Nanoscale Res. Lett.* **11** 453
[16] Lee S J, Kim S H, Kim D W, Kim K H, Kim B K and Jang J 2011 *Sol. Energ. Mat. Sol. C.* **95** 81
[17] Martinuzzi S, Périchaud I and Warchol F 2003 *Sol. Energ. Mat. Sol. C* **80** 343
[18] Lüdemann R 1999 *Materials Science and Engineering: B* **58** 86
[19] Hu Z H, Liao X B, Liu Z M, Xia C F and Chen T J 2003 *Chin. Phys.* **12** 112
[20] Descoeudres A, Barraud L, De Wolf S, Strahm B, Lachenal D, Guérin C, Holman Z C, Zicarelli F, Demaurex B and Seif J 2011 *Appl. Phys. Lett.* **99** 123506
[21] Martin I, Vetter M, Orpella A, Voz C, Puigdollers J, Alcubilla R, Kharchenko A V and Roca I Cabarrocas P 2004 *Appl. Phys. Lett.* **84** 1474
[22] Gorka B, Rau B, Dogan P, Becker C, Ruske F, Gall S and Rech B 2009 *Plasma Process. Polym.* **6** S36
[23] Wang F, Zhang X, Wang L, Jiang Y, Wei C, Sun J and Zhao Y 2014 *ACS Appl. Mater. Inter.* **6** 15098
[24] Seager C H and Ginley D S 1981 *J. Appl. Phys.* **52** 1050
[25] Do Kim Y, Park S, Song J, Tark S J, Kang M G, Kwon S, Yoon S and Kim D 2011 *Sol. Energ. Mat. Sol. C* **95** 73
[26] Qiu Y, Kunz O, Fejfar A, Ledinsky M, Chan B T, Gordon I, Van Gestel D, Venkatachalm S and Egan R 2014 *Sol. Energ. Mat. Sol. C* **122** 31
[27] Wang X Q, Yang D R, Xi Z Q and Que D L 2002 *Semiconductor Photonics and Technology* **8** 228
[28] Wang D C, Zhang C, Zeng P, Zhou W, Ma L, Wang H, Zhou Z, Hu F, Zhang S and Lu M 2018 *Sci. Bull.* **63** 75
[29] Zhang C, Zeng P, Zhou W, Zhang Y, He X, Jin Q, Wang D, Wang H, Zhang S, Lu M and Wu X 2019 *IEEE J. Selec. Top. Quantum Electron.* **26** 1
[30] Zhang X, Liu B W, Xia Y, Li C B, Liu J and Shen Z N 2012 *Acta Phys. Sin.* **61** 444 (in Chinese)
[31] Lee M C M and Wu M C 2006 *Journal of Microelectromechanical Systems 15* 338
[32] Habuka H, Tsunoda H, Mayusumi M, Tate N and Katayama M 1995 *J. Electrochem. Soc.* **142** 3092
[33] Murakami K, Fukata N, Sasaki S, Ishioka K, Kitajima M, Fujimura S, Kikuchi J and Haneda H 1996 *Phys. Rev. Lett.* **77** 3161
[34] van de Walle C G and Nickel N H 1995 *Phys. Rev. B* **51** 2636
[35] Kim K, Varlamov S, Evans R and Egan R 2013 *IEEE 39th Photovoltaic Specialists Conference (PVSC)*, 16–21 June, 2013, Tampa, FL, USA, p. 0568
[36] Sassella A, Borghesi A, Corni F, Monelli A, Ottaviani G, Tonini R, Pivac B, Bacchetta M and Zanotti L 1997 *Journal of Vacuum Science & Technology A* **15** 377
[37] Cortazar O, Aceves M, Yu Z and Kiebach R 2009 *6th International Conference on Electrical Engineering, Computing Science and Automatic Control (CCE)*, 10–13 Jan. 2009, Toluca, Mexico, pp. 1–5
[38] Van de Walle C G 1994 *Phys. Rev. B* **49** 4579
[39] Zhang Y C, Zhang C, Li S, Dai X Y, Ma X F, Gao R H, Zhou W J and Lu M 2020 *Opt. Express* **28** 23320
[40] Syed Ahamed Basheer M G, Rajni K S, Vidhya V S, Swaminathan V, Thayumanavan A, Murali K R and Jayachandran M 2011 *Crystal Research & Technology* **46** 261
[41] Hsu C L and Lu Y C 2012 *Nanoscale* **4** 5710
[42] Yang L, Wang Z H and Zhang Z D 2016 *J. Appl. Phys.* **119** 045304